IRSTI 27.35.19 https://doi.org/10.26577/ijmph.202516110

S.M. Lamtiuhova

Kharkiv National University of Radio Electronics, Nauky Ave. 14, Kharkiv, Ukraine,
*e-mail: svitlana.lamtiuhova@nure.ua

(Received 20 January 2025; revised 25 May 2025; accepted 1 June 2025)

Mathematical Modeling of Steady Flow Past Circular Cylinder with Splitter Plates by R-Functions Method

Abstract. In the paper the steady flow of a viscous incompressible fluid past a circular cylinder with attached splitter plates is considered. The mathematical representation of the problem takes the form of an external boundary value problem for the stream function. To solve the problem, a numerical method combining the *R*-functions and the nonlinear Galerkin method is used. The *R*-functions method is employed to construct a problem solution structure that exactly satisfies all the boundary conditions of the problem and has the required behavior at infinity. The Galerkin method is then applied to approximate the undetermined components of this structure, ensuring accuracy and efficiency in the solution process. A series of computational experiments was conducted to investigate the flow past a single circular cylinder and past a circular cylinder with triangular and rectangular splitter plates at various Reynolds numbers. For the case of a single cylinder, a quantitative error analysis confirms the convergence of the numerical method, with relative errors dropping below 1% when using a moderate number of basis functions. The computational cost remains practical, with each solution obtained in approximately 11 minutes on a standard workstation. Drag and lift coefficients are computed for the single-cylinder case, allowing for quantitative assessment of aerodynamic performance and validation of the numerical model against known reference data. The influence of splitter plate geometry on the flow structure is explored through visualizations, highlighting changes in vortex patterns and symmetry. The proposed approach demonstrates strong numerical accuracy and computational robustness for the single-cylinder case and offers a flexible framework for studying external viscous flows with complex boundary configurations.

Keywords: Viscous incompressible fluid, External boundary value problem, Stream function, *R*-functions method, Nonlinear Galerkin method.

Introduction

Mathematical modeling and numerical analysis play a significant role in investigating and solving applied problems by simulating the behavior of complex systems in diverse areas. They are used in hydrodynamics, thermal energy, chemical kinetics, biomedicine, material science, engineering, and even medical diagnostics [1–4].

One of these important areas is the dynamics of viscous fluids, which studies fluid flow behavior and is relevant to numerous industrial and environmental applications. Accurate modeling of viscous fluid behavior, particularly around bodies of various shapes, is essential for understanding processes such as vortex formation, wake dynamics, and flow stability. These insights are fundamental to advancing technologies in engineering, energy, and other fields [5–8].

It is well known that at low Reynolds numbers the flow around a body remains symmetrical, with no detachment zone forming in the wake region. As the Reynolds number increases, secondary vortices appear behind the body. These vortices grow in size due to the energy of the flow and after reaching a certain (critical) value eventually detach from the body. When flow conditions favor the formation of a well-defined vortex street, a cross flow appears directly behind the body, with a component perpendicular to the direction of the incoming flow. Installing a splitter plate into the near trace created by the body can effectively suppress or reduce the formation of such vortex streets, stabilizing the flow.

Splitter plates, often called as wake stabilizers, are introduced downstream of a body. They are passive means to regulate various aspects of wake formation and mitigate vortex shedding. The use of these plates makes it possible to change the pressure

drop characteristics. The resistance to the body can be reduced when the flow reattaches downstream, thereby making it streamlined. A variety of splitter plate configurations can be used, each tailored to specific flow control objectives. Shrivastava et al. [9] investigated the flow around a circular cylinder and cylinders with triangular and rectangular wake splitter plates using an incompressible PISO finite volume method. Their approach employed a non-staggered grid arrangement and a second-order upwind scheme for the convective terms.

This paper aims to apply the *R*-functions and nonlinear Galerkin method for mathematical modeling of a nonlinear steady-state problem of viscous incompressible fluid flow past a circular cylinder with triangular and rectangular splitter plates. The problem has symmetrical properties and can be simplified to a two-dimensional form, making the stream function more convenient to use than the fluid velocity components. The methods for solving external problems for the equation related to the stream function have not been sufficiently developed, primarily because of the equation's high order, nonlinearity and the unbounded domain in which it is considered. By employing the constructive tools from *R*-functions theory, it becomes possible to accurately account for the geometry of the domain and all boundary conditions, including the condition at infinity.

The *R*-functions method is a powerful tool for solving a wide class of problems in mathematical physics and mechanics, including problems in hydrodynamics. This method, originally introduced by the Ukrainian mathematician V. L. Rvachov, relies on the use of special functions that preserve the logical structure of geometric domains and physical conditions [10, 11]. In hydrodynamics, it is used to model fluid flows in channels and reservoirs with complex geometries, solve free liquid surface problems, analyze heat transfer in pipes with intricate cross-sections, and study magnetohydrodynamic flows.

Maksymenko-Sheiko et al. examined conjugate boundary-value problems related to heat transfer in fuel cartridges containing fuel rods, emphasizing cases where a viscous incompressible fluid moves through channels with non-standard cross-sections, flowing around a rods bundle [12, 13]. It was also investigated situations involving asymmetrical rod arrangements [14] and explored a variety of finned fuel elements surfaces including polyzonal finning of the shell [15]. Podhornyj et al. [16] considered stationary fluid flow through a piecewise homogeneous porous medium, assuming the applicability of Darcy's law. The mathematical modeling of a quasi-stationary mixing process of a viscous mixture was investigated by Gybkina et al. [17] using a combination of the superposition principle, the *R*-functions method, and the Ritz variational method. In the context of external flow problems around bodies, the *R*-functions method has been applied in [18–21], considering cases such as flow around bodies of revolution in spherical coordinates, flow past cylindrical bodies without splitter plates, and mass exchange problems.

The problems of flow around bodies attract considerable attention due to their wide range of industrial and engineering applications. Examples of interesting applications of flows past cylinders of various shapes include flows around tall chimneys, cooling towers, offshore structures, pipelines, bridges, rod bundles in heat exchangers, and flame stabilizers in high-speed combustion chambers.

Problem statement

Consider the steady, uniform flow of viscous incompressible fluid past a cylindrical body, with a velocity at infinity U_∞. The cross-section of the body is a finite domain Ξ with a piecewise-smooth boundary $\partial\Xi$. Let Ω be complement of $\overline{\Xi}$. It is clear that $\partial\Omega = \partial\Xi$. It is convenient to consider such flows in a cylindrical coordinate system (r, φ, z). Assume that all quantities describing the flow are independent of the coordinate z and that the third component of the fluid velocity is equal to zero, i.e. $V_z = 0$. The stationary Navier-Stokes equations then take the following form [6]:

$$\begin{aligned} &V_r\frac{\partial V_r}{\partial r}+\frac{V_\varphi}{r}\frac{\partial V_r}{\partial \varphi}-\frac{V_\varphi^2}{r}= \\ &=-\frac{1}{\rho}\frac{\partial P}{\partial r}+\nu\left(\Delta V_r-\frac{V_r}{r^2}-\frac{2}{r^2}\frac{\partial V_\varphi}{\partial \varphi}\right), \\ &V_r\frac{\partial V_\varphi}{\partial r}+\frac{V_\varphi}{r}\frac{\partial V_\varphi}{\partial \varphi}+\frac{V_rV_\varphi}{r}= \\ &=-\frac{1}{\rho}\frac{1}{r}\frac{\partial P}{\partial \varphi}+\nu\left(\Delta V_\varphi+\frac{2}{r^2}\frac{\partial V_r}{\partial \varphi}-\frac{V_\varphi}{r^2}\right), \end{aligned} \qquad (1)$$

$$\frac{\partial\left(rV_r\right)}{\partial r}+\frac{\partial V_\varphi}{\partial\varphi}=0,$$

where:

$\Delta=\frac{\partial^2}{\partial r^2}+\frac{1}{r}\frac{\partial}{\partial r}+\frac{1}{r^2}\frac{\partial^2}{\partial\varphi^2}$ is Laplace operator;

V_r, V_φ are fluid velocity components;

P is pressure;

$\nu=\mathrm{Re}^{-1}$ is kinematic viscosity coefficient;

Re is Reynolds number;

ρ is fluid density.

The system of equations (1) consists of nonlinear partial differential equations for the unknown functions V_r, V_φ, P.

The third equation in (1), the continuity equation, is integrated by introducing the stream function ψ according to formulas [5, 22]:

$$V_r=\frac{1}{r}\frac{\partial\psi}{\partial\varphi},\ V_\varphi=-\frac{\partial\psi}{\partial r}.$$

Elimination of the pressure from the two remaining equations via cross-differentiation leads to a nonlinear fourth-order equation for the stream function $\psi=\psi(r,\varphi)$ [22]:

$$\nu\Delta^2\psi=\frac{1}{r}\frac{\partial\psi}{\partial\varphi}\frac{\partial(\Delta\psi)}{\partial r}-\frac{1}{r}\frac{\partial\psi}{\partial r}\frac{\partial(\Delta\psi)}{\partial\varphi}\ \text{ in }\Omega,\quad(2)$$

where:

$$\Delta\psi=\frac{1}{r}\frac{\partial}{\partial r}\left(r\frac{\partial\psi}{\partial r}\right)+\frac{1}{r^2}\frac{\partial^2\psi}{\partial\varphi^2};$$

$$\Delta^2\psi=\Delta\left(\Delta\psi\right).$$

Equation (2) should be complemented with boundary conditions on $\partial\Omega$ and the condition at infinity (for $r\to+\infty$) [5, 6]:

$$\psi\big|_{\partial\Omega}=0,\ \left.\frac{\partial\psi}{\partial\mathbf{n}}\right|_{\partial\Omega}=0,\quad(3)$$

$$\lim_{r\to+\infty}r^{-1}\psi=U_\infty\sin\varphi,\quad(4)$$

where:

$\mathbf{n}$ is external normal to $\partial\Omega$.

Method of solving the problem (2) – (4)

As proven in [19], for any sufficiently smooth functions Φ_1 and Φ_2 (with $\Phi_1\cdot r^{-1}\to 0$ as $r\to+\infty$), the boundary conditions (3) and the condition at infinity (4) are exactly satisfied by a function of the form:

$$\psi=\omega_M^2(\psi_0+\Phi_1)+\omega_M^2(1-\omega_M)\Phi_2,$$

where:

$\psi_0=U_\infty\left(r-\frac{R^2}{r}\right)\sin\varphi$ is the solution to the problem of flow past a circular cylinder of radius R by an ideal fluid (the cylinder of radius R is fully contained within the streamlined body);

$$\omega_M=f_M(\omega)=\begin{cases}1-\exp\dfrac{M\omega}{\omega-M}, & 0\le\omega<M;\\ 1, & \omega\ge M\ (M=\mathrm{const}>0),\end{cases}\quad(5)$$

where:

$\omega(r,\varphi)$ is the function that satisfies the following conditions:

a) $\omega(r,\varphi)>0$ in Ω, b) $\omega(r,\varphi)\big|_{\partial\Omega}=0$,

c) $\left.\frac{\partial\omega}{\partial\mathbf{n}}\right|_{\partial\Omega}=-1$.

The function (5) differs from unity only in a finite annular region $\{0\le\omega(r,\varphi)<M\}$ adjacent to the contour $\partial\Omega$, as it satisfies the following conditions:

1) $\omega_M>0$ in Ω, 2) $\omega_M\big|_{\partial\Omega}=0$,

3) $\left.\frac{\partial\omega_M}{\partial\mathbf{n}}\right|_{\partial\Omega}=-1$, 4) $\omega_M\equiv 1$, if $\omega_M\ge M$.

Thus, the function (5) allows for calculations within the finite region.

The functions Φ_1 and Φ_2 are approximated using the nonlinear Galerkin method [8] in the following form:

$$\Phi_1 = \sum_{k=1}^{m_1} \alpha_k \cdot \varphi_k \,,\ \Phi_2 = \sum_{j=1}^{m_2} \beta_j \cdot \tau_j \,,$$

where:

$$\left\{\varphi_k(r,\varphi)\right\} = \left\{ r^{-k} \begin{matrix}\cos k\varphi \\ \sin k\varphi\end{matrix}, k = 1,2,...;\ r^{2-k} \begin{matrix}\cos k\varphi \\ \sin k\varphi\end{matrix}, k = 3,4,... \right\}$$

is a complete set of particular solutions to the equation $\Delta^2 u = 0$ for the region outside a finite-radius cylinder;

$$\left\{\tau_j(r,\varphi)\right\} = \left\{ \cos 2\varphi,\ \sin 2\varphi,\ r^j \begin{matrix}\cos j\varphi \\ \sin j\varphi\end{matrix},\ r^{j+2} \begin{matrix}\cos j\varphi \\ \sin j\varphi\end{matrix}, j = 1,2,... \right\}$$

is a complete set of particular solutions to the equation $\Delta^2 u = 0$ for the domain $\left\{\omega(r,\varphi) < M\right\}$.

Hence, the problem's solution is approximated in the form:

$$\psi_N = \omega_M^2 \left(U_\infty \left(r - \frac{R^2}{r} \right) \sin\varphi + \sum_{k=1}^{m_1} \alpha_k \cdot \varphi_k \right) + \omega_M^2 (1 - \omega_M) \sum_{j=1}^{m_2} \beta_j \cdot \tau_j \,.$$

The complete sequence of functions for the whole plane is expressed as:

$$\left\{\varphi_i(r,\varphi)\right\} = \left\{\omega_M^2(r,\varphi)\varphi_k(r,\varphi),\ \omega_M^2(r,\varphi)(1-\omega_M(r,\varphi))\tau_j(r,\varphi)\right\}. \quad (6)$$

The nonlinear Galerkin method [8] is employed to determine the unknown coefficients α_k $(k = 1,2,...,m_1)$ and β_j $(j = 1,2,...,m_2)$ by enforcing the orthogonality condition of the residual to the first N $(N = m_1 + m_2)$ elements of the sequence (6):

$$\left(\nu\Delta^2\psi_N - \frac{1}{r}\frac{\partial\psi_N}{\partial\varphi}\frac{\partial(\Delta\psi_N)}{\partial r} + \frac{1}{r}\frac{\partial\psi_N}{\partial r}\frac{\partial(\Delta\psi_N)}{\partial\varphi}, \varphi_i \right) = 0\,,\ i = \overline{1,N}\,.$$

The resulting system consists of nonlinear equations, each being a quadratic function of the unknown coefficients α_k and β_j. The system can be solved using the Newton method. For the initial approximation, a set of α_k and β_j, corresponding to the solution of the Oseen problem, or for large Reynolds numbers, a solution obtained from smaller Reynolds numbers, should be selected.

Results and discussions

A computational experiment was conducted for the problems of flow past a single circular cylinder and past a circular cylinder with triangular and rectangular splitter plates at $U_\infty = 1$, $M = 5$, $m_1 = 8$, $m_2 = 14$, $\mathrm{Re} = 5;10;15$.

In the case of flow past a single circular cylinder $x^2 + y^2 = 1$, the normalized equation of the boundary [10, 11] takes the following form:

$$\omega(x,y) = \frac{1}{2}(1 - x^2 - y^2) = 0\,.$$

Figure 1 illustrates the streamline contours of the approximate solution for the steady flow past a circular cylinder at various Reynolds numbers ($\mathrm{Re} = 5;10;15$). The contours remain symmetric

with respect to the horizontal axis across all tested Reynolds numbers, but a clear evolution of the wake structure is observed. As Re increases, the separation region behind the cylinder becomes more elongated, and closed recirculation zones form in the near wake. This behavior reflects the growing influence of inertial forces over viscous effects. Figure 2 complements the picture by presenting the velocity vector fields superimposed on the streamline contours. At $\mathrm{Re}=5$, the flow is smooth with only a short wake, while at $\mathrm{Re}=10$ and especially at $\mathrm{Re}=15$, recirculation zones develop behind the cylinder, becoming more prominent and spatially extended. The results are consistent with expected trends for laminar flow past bluff bodies, where increasing Reynolds number leads to stronger velocity gradients and the onset of vortex-like behavior.

For two successive approximate solutions constructed with $N_k = m_1 + m_2$ basic functions by Galerkin method the following calculation errors were evaluated:

– absolute deviation:

$$\Delta_k = \max\left|\psi_{N_{k+1}}(r,\theta) - \psi_{N_k}(r,\theta)\right|,$$

– L_2-norm: $\Delta = \left\|\psi_{N_{k+1}}(r,\theta) - \psi_{N_k}(r,\theta)\right\|_{L_2(\Omega)}$,

– relative error:

$$\delta = \frac{\left\|\psi_{N_{k+1}}(r,\theta) - \psi_{N_k}(r,\theta)\right\|_{L_2(\Omega)}}{\left\|\psi_{N_k}(r,\theta)\right\|_{L_2(\Omega)}}.$$

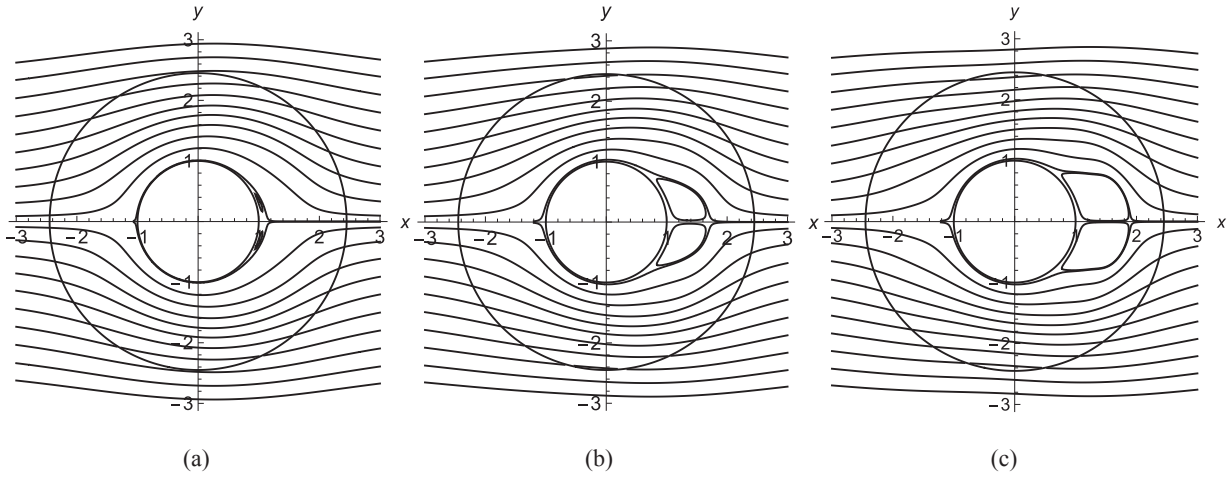

(a) (b) (c)

Figure 1 – The streamline contours for the problem of flow past a circular cylinder at (a) $\mathrm{Re}=5$, (b) $\mathrm{Re}=10$, (c) $\mathrm{Re}=15$.

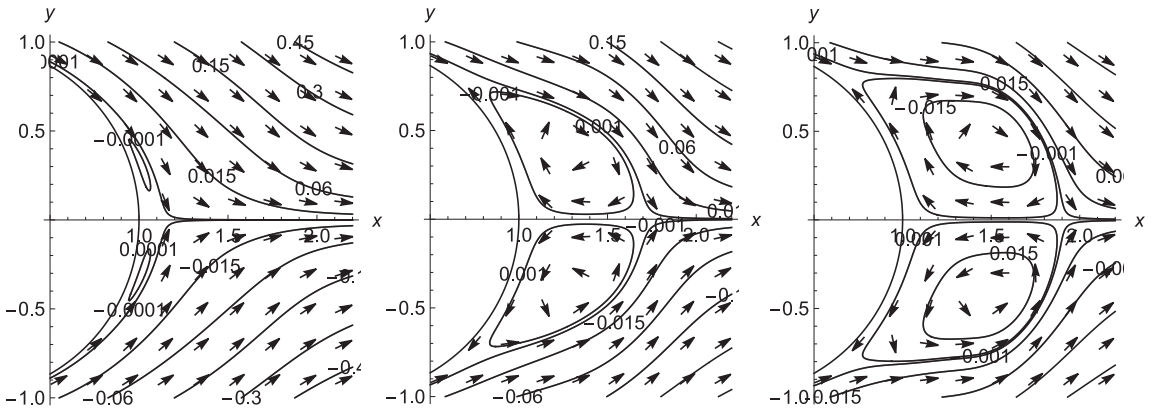

(a) (b) (c)

Figure 2 – Detailed visualizations of the streamline contours and velocity vector fields behind the circular cylinder at (a) $\mathrm{Re}=5$, (b) $\mathrm{Re}=10$, (c) $\mathrm{Re}=15$

Table 1 presents the computational errors at $M = 5$ for pairs of approximate solutions computed with different values of N_k. The numerical results demonstrate the convergence properties of the Galerkin method applied to the problem of viscous flow past a circular cylinder. The analysis of computational errors confirms that increasing the number of basis functions $N_k = m_1 + m_2$ improves the accuracy of the approximate solutions.

It is observed that using 22 basis functions yields sufficiently accurate results for all tested Reynolds numbers, with relative errors dropping to around or below 1%. Increasing the number of basic functions to 30 leads to only marginal improvements in accuracy. Therefore, from a computational efficiency perspective, the choice of 22 basis functions provides a good balance between accuracy and computational cost. The computational cost remains moderate, with each solution requiring approximately 11 minutes on a standard workstation (Intel i5 processor, 8 GB RAM). For higher Reynolds numbers, however, a larger number of basis functions may be necessary to maintain the same level of accuracy due to the increased complexity of the flow field.

These findings confirm that the Galerkin method offers a convergent and computationally feasible approach for solving this class of fluid dynamics problems, with controllable accuracy through a moderate number of basis functions.

The obtained results show good agreement with experimental data available in the literature [7], as well as with the findings of other researchers [6, 23, 24] and with those presented in [20], which were derived using the *R*-functions, successive approximations, and the Galerkin method. The secondary vortices behind the body emerge as the Reynolds number reaches 5, consistent with previously known results and highlighting the efficiency of the developed numerical method.

Table 1 – Computational errors at $M = 5$ for successive Galerkin approximations with increasing number of basic functions N_k.

N_k, N_{k+1}	**Type of error**	**Re = 5**	**Re = 10**	**Re = 15**
$N_1 = 2 + 4 = 6$ $N_2 = 4 + 10 = 14$	Δ_k	$0{,}12 \times 10^{0}$	$0{,}25 \times 10^{0}$	$0{,}37 \times 10^{0}$
	Δ	$0{,}26 \times 10^{0}$	$0{,}49 \times 10^{0}$	$0{,}68 \times 10^{0}$
	δ	9,5%	18,3%	25,4%
$N_2 = 4 + 10 = 14$ $N_3 = 8 + 14 = 22$	Δ_k	$0{,}55 \times 10^{-1}$	$0{,}20 \times 10^{0}$	$0{,}35 \times 10^{0}$
	Δ	$0{,}99 \times 10^{-1}$	$0{,}32 \times 10^{0}$	$0{,}55 \times 10^{0}$
	δ	3,7%	11,6%	18,9%
$N_3 = 8 + 14 = 22$ $N_4 = 12 + 18 = 30$	Δ_k	$0{,}11 \times 10^{-1}$	$0{,}70 \times 10^{-1}$	$0{,}14 \times 10^{0}$
	Δ	$0{,}12 \times 10^{-2}$	$0{,}54 \times 10^{-2}$	$0{,}10 \times 10^{-1}$
	δ	0,05%	0,2%	0,4%

Having demonstrated that the Galerkin solution is sufficiently accurate and computationally efficient, we now apply it to compute the drag and lift coefficients. These quantities are of primary interest in external flow problems and serve as key metrics for validating numerical predictions against experimental or benchmark data.

Drag F_D and lift F_L forces, acting from the fluid side to the cylinder, can be calculated using the formulas [5, 8, 25]:

$$F_D = \int_S (-\tau_{rr} \cos\varphi + \tau_{r\varphi} \sin\varphi) ds,$$

$$F_L = \int_S (-\tau_{rr} \sin\varphi - \tau_{r\varphi} \cos\varphi) ds,$$

where:

S is the surface of the cylinder;

τ_{rr}, $\tau_{r\varphi}$ are stresses on the cylinder surface:

$$\tau_{rr} = \left(-p + 2\nu \frac{\partial u_r}{\partial r} \right)\Big|_S,$$

$$\tau_{r\varphi} = \nu \left(\frac{\partial u_\varphi}{\partial r} - \frac{u_\varphi}{r} + \frac{1}{r} \frac{\partial u_r}{\partial \varphi} \right)\Big|_S.$$

According to the Navier–Stokes equations (1):

$$\frac{\partial p}{\partial r} = -\rho\left(V_r\frac{\partial V_r}{\partial r} + \frac{V_\varphi}{r}\frac{\partial V_r}{\partial \varphi} - \frac{V_\varphi^2}{r}\right) + \\ +\rho\nu\left(\Delta V_r - \frac{V_r}{r^2} - \frac{2}{r^2}\frac{\partial V_\varphi}{\partial \varphi}\right),$$

$$\frac{1}{r}\frac{\partial p}{\partial \varphi} = -\rho\left(V_r\frac{\partial V_\varphi}{\partial r} + \frac{V_\varphi}{r}\frac{\partial V_\varphi}{\partial \varphi} + \frac{V_r V_\varphi}{r}\right) + \\ +\rho\nu\left(\Delta V_\varphi + \frac{2}{r^2}\frac{\partial V_r}{\partial \varphi} - \frac{V_\varphi}{r^2}\right).$$

Then the pressure can be found by integrating the following expression:

$$dp = \frac{\partial p}{\partial r}dr + \frac{\partial p}{\partial \varphi}d\varphi.$$

The drag C_D and lift C_L coefficient can be defined as [5, 8, 25]

$$C_D = \frac{F_D}{\frac{1}{2}\rho A U_\infty^2},\ C_L = \frac{F_L}{\frac{1}{2}\rho A U_\infty^2},$$

where:

A is the projected area.

To compare our obtained drag coefficients, let us consider the folowing empirical expressions for the drag coefficient of flow past a cylinder [26]:

Wieselsberger-Lamb: $C_D = \dfrac{8\pi}{\mathrm{Re}(2{,}002 - \lg \mathrm{Re})}$,

Clift: $C_D = \dfrac{24(1 + 0{,}15\,\mathrm{Re}^{0{,}687})}{\mathrm{Re}}$,

Munson: $C_D = \dfrac{5{,}93}{\sqrt{\mathrm{Re}}} + 1{,}17$.

The obtained approximate drag coefficients have been compared with the empirical correlations mentioned above, as well as with the numerical results reported by other researchers, as presented in Table 2.

The comparison of drag coefficients obtained in the present study with well-known empirical correlations demonstrates the validity and accuracy of the developed numerical model in the low Reynolds number regime. At $\mathrm{Re} = 5$, the drag coefficient from the present work shows good agreement with the values predicted by Wieselsberger-Lamb and Clift, indicating that the model correctly captures the viscous-dominated flow behavior. For $\mathrm{Re} = 10$, the computed drag coefficient closely matches the empirical estimate given by Clift, and for $\mathrm{Re} = 15$, it aligns well with the estimate provided by Munson. This consistency further supports the robustness and reliability of the numerical approach used in this study.

Table 2 – Drag coefficients for flow past a single circular cylinder at $\mathrm{Re} = 5;10;15$

Authors	Re = 5	Re = 10	Re = 15
Wieselsberger-Lamb	8,80	2,50	1,46
Clift	6,98	4,15	3,14
Munson	3,82	3,05	2,70
Perumal [23]	-	3,21	-
Silva [27]	-	2,81	-
Shrivastava [9]	5,92	-	-
Mehmet [28]	-	-	3,08
Present work	7,95	4,05	2,74

Notably, the Wieselsberger-Lamb formula tends to overestimate the drag at low Reynolds numbers, while the Munson and Clift correlations provide more consistent results across the considered range. The comparison also shows a general trend of decreasing with increasing Reynolds number, as

expected due to the diminishing relative effect of viscosity.

In addition, the lift coefficient $C_L = 0$ computed in the present study was found to be zero, which is consistent with the symmetric geometry and boundary conditions of the problem. This result further confirms the physical correctness of the numerical solution and the ability of the method to preserve expected flow symmetries.

Overall, the present numerical results exhibit good agreement with both empirical models and available data in the literature, confirming the applicability of the method for simulating creeping and transitional flows around a circular cylinder.

Consider the problem of flow past a circular cylinder $x^2 + y^2 = 1$ with a triangular splitter plate (Figure 3).

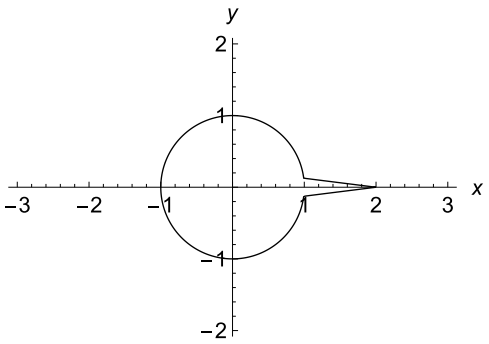

Figure 3 – Circular cylinder with a triangular splitter plate

Let us construct a normalized boundary equation using the *R*-functions system R_0 [10, 11, 18]:

$$\overline{x} \equiv -x\,,\ x \wedge_0 y \equiv x + y - \sqrt{x^2 + y^2}$$
$$x \vee_0 y \equiv x + y + \sqrt{x^2 + y^2}\,. \qquad (7)$$

The following regions are accepted as primitive regions:

– the interior of a circle with a radius of 1 and centered at the origin: $\Sigma_1 = \left(\frac{1}{2}\left(1 - x^2 - y^2\right) \ge 0\right)$,

– the half-plane below the line $x + 8y - 2 = 0$: $\Sigma_2 = \left(\frac{1}{\sqrt{65}}\left(2 - x - 8y\right) \ge 0\right)$,

– the half-plane above the line $x - 8y - 2 = 0$: $\Sigma_3 = \left(\frac{1}{\sqrt{65}}\left(2 - x + 8y\right) \ge 0\right)$,

– the half-plane to the right of the line $x = \frac{1}{2}$: $\Sigma_4 = \left(x - \frac{1}{2} \ge 0\right)$.

Then $\overline{\Omega} = \Sigma_1 \vee \left(\Sigma_2 \wedge \Sigma_3 \wedge \Sigma_4\right)$ and the equation of the boundary of the region Ω is determined by the equation $\omega(x, y) = 0$, where

$$\omega(x, y) = \left[\frac{1 - x^2 - y^2}{2}\right] \vee_0 \left(\left[\frac{2 - x - 8y}{\sqrt{65}}\right] \wedge_0 \left[\frac{2 - x + 8y}{\sqrt{65}}\right] \wedge_0 \left[x - \frac{1}{2}\right]\right). \qquad (8)$$

The function (8) is positive within the domain Ω and negative outside of Ω. If a function that is positive in the exterior of the finite domain Ω is required, one should use the function $-\omega(x, y)$.

Figure 4 illustrates the streamline contours of the approximate solution for the case of flow past a circular cylinder with a triangular splitter plate. Figure 5 provides a more detailed view, combining these contours with the velocity vector fields behind the body. The presence of the triangular splitter plate significantly modifies the near-wake structure. Across all considered Reynolds numbers, the flow retains its symmetry, but the splitter effectively confines and redirects the flow in the wake region. As a result, the separated region behind the cylinder becomes narrower and more confined, indicating a stabilizing effect of the plate and a potential reduction in unsteady vortex formation.

Consider the problem of flow past a circular cylinder $x^2 + y^2 = 1$ with a rectangular splitter plate (Figure 6).

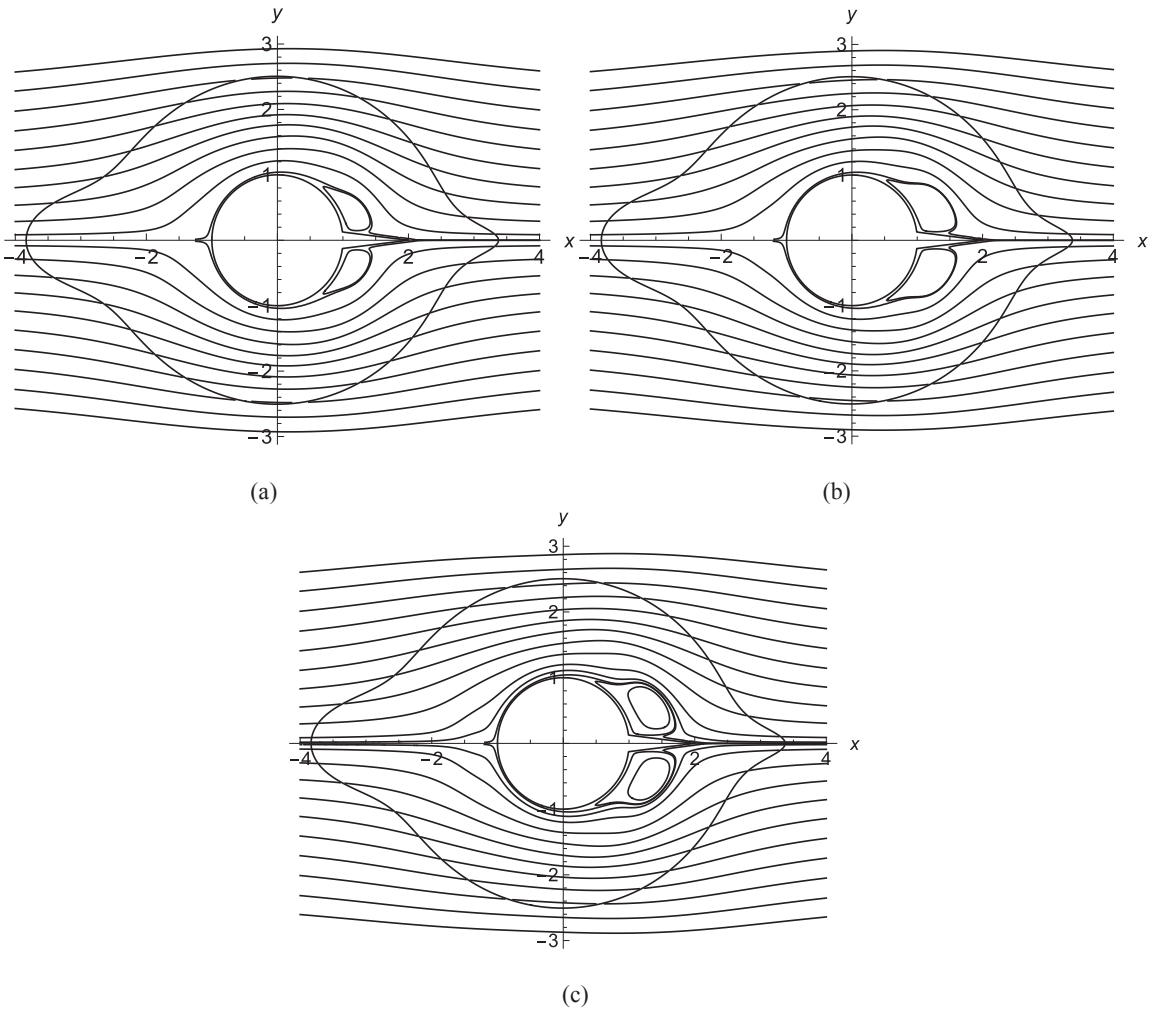

Figure 4 –The streamline contours for the problem of flow past a circular cylinder with a triangular splitter plate at (a) $\mathrm{Re} = 5$, (b) $\mathrm{Re} = 10$, (c) $\mathrm{Re} = 15$

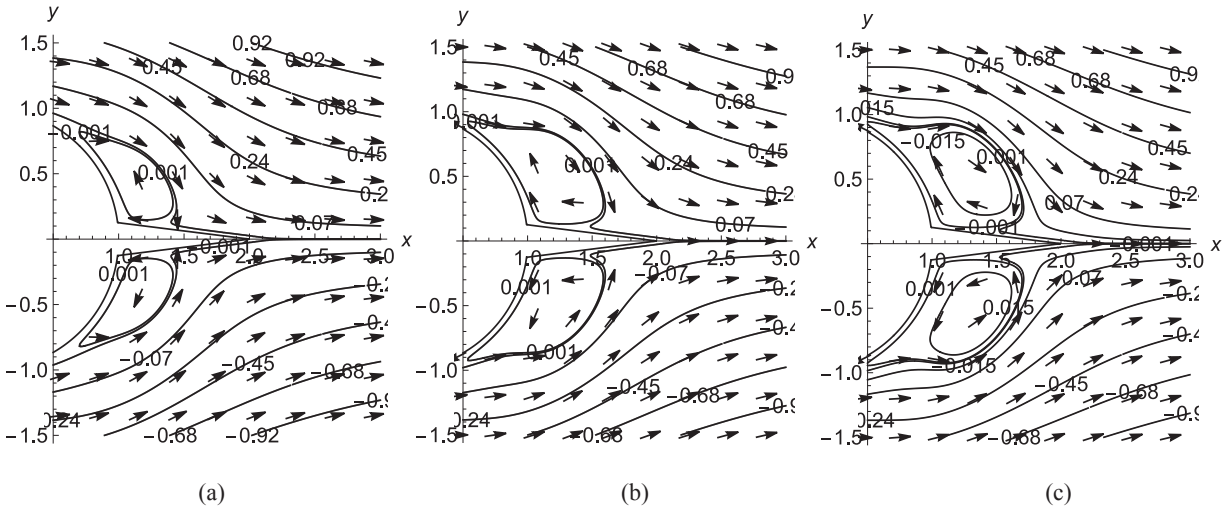

Figure 5 – Detailed visualizations of the streamline contours and velocity vector fields behind the circular cylinder with a triangular splitter plate at (a) $\mathrm{Re} = 5$, (b) $\mathrm{Re} = 10$, (c) $\mathrm{Re} = 15$

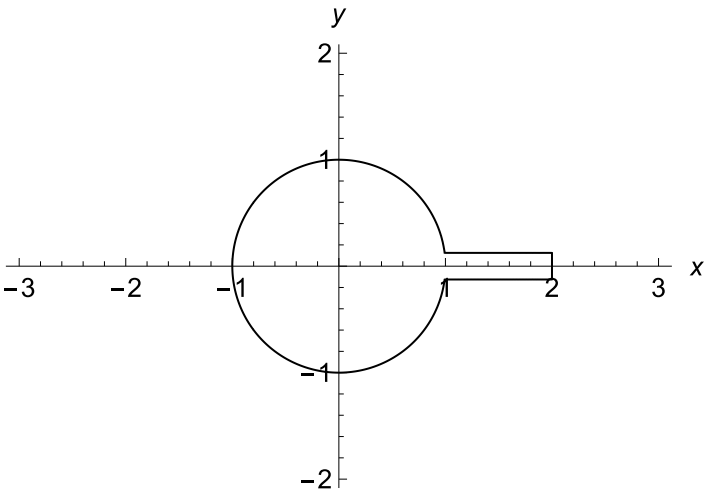

Figure 6 – Circular cylinder with a rectangular splitter plate

To construct a normalized boundary equation [10, 11, 18] using the *R*-functions system R_0 (7), we considered the following primitive regions:

– the interior of a circle of radius 1 centered at the origin: $\Sigma_1 = \left(\frac{1}{2}\left(1 - x^2 - y^2\right) \geq 0\right)$,

– the half-plane below the line $y - \frac{1}{8} = 0$: $\Sigma_2 = \left(\frac{1}{8} - y \geq 0\right)$,

– the half-plane above the line $y + \frac{1}{8} = 0$: $\Sigma_3 = \left(\frac{1}{8} + y \geq 0\right)$,

– the half-plane to the right of the line $x = \frac{1}{2}$: $\Sigma_4 = \left(x - \frac{1}{2} \geq 0\right)$,

– the half-plane to the left of the line $x = 2$: $\Sigma_5 = \left(2 - x \geq 0\right)$.

Then $\overline{\Omega} = \Sigma_1 \vee \left(\Sigma_2 \wedge \Sigma_3 \wedge \Sigma_4 \wedge \Sigma_5\right)$ and the equation of the boundary of the region Ω is determined by the equation $\omega(x, y) = 0$, where

$$\omega(x,y) = \left[\frac{1 - x^2 - y^2}{2}\right] \vee_0 \left(\left[\frac{1}{8} - y\right] \wedge_0 \left[\frac{1}{8} + y\right] \wedge_0 \left[x - \frac{1}{2}\right] \wedge_0 \left[2 - x\right]\right). \quad (9)$$

The constructed function (9) is also positive within the domain Ω and negative outside Ω.

The streamline contours of the obtained approximate solution for the case of flow past a circular cylinder with a rectangular splitter plate, as well as detailed pictures of these contours and velocity vector fields behind the body, are presented in Figures 7 and 8. Compared to the triangular configuration, the rectangular plate more effectively suppresses wake expansion, especially at Re=15, where the flow behind the cylinder remains relatively attached and streamlined. The splitter reduces the tendency of the flow to separate sharply, thereby weakening recirculation and mitigating vortex development.

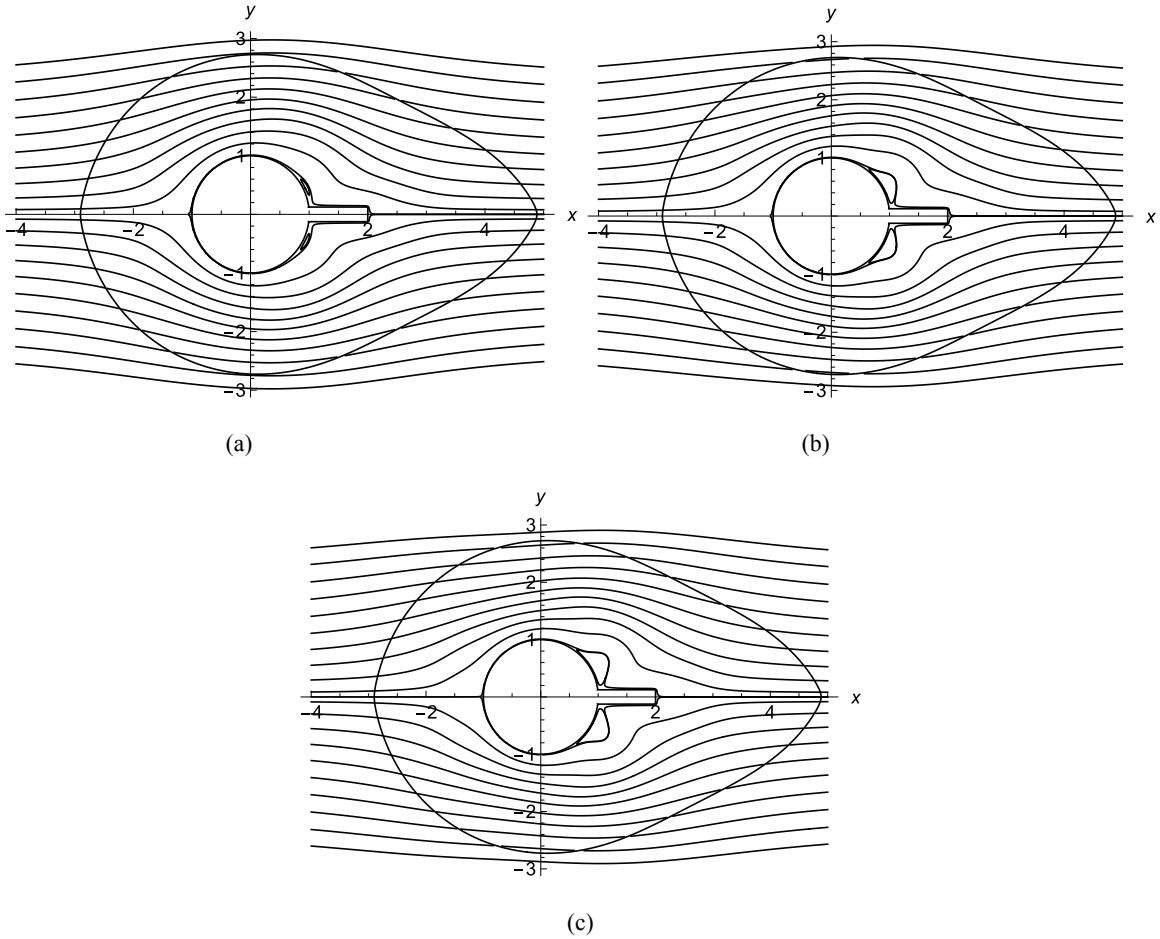

Figure 7 – The streamline contours for the problem of flow past a circular cylinder with a rectangular splitter plate at (a) $\mathrm{Re} = 5$, (b) $\mathrm{Re} = 10$, (c) $\mathrm{Re} = 15$

Conclusions

The paper presents the application of the *R*-functions and nonlinear Galerkin method to the mathematical modeling of the nonlinear stationary problem of viscous incompressible fluid flow past a cylindrical body. The use of R-functions enables the construction of an approximate solution in the form of a single analytical expression that inherently satisfies the boundary conditions and captures the geometry of the domain precisely. Numerical solutions were obtained for the nonlinear stationary problem of flow past both a single circular cylinder and a circular cylinder with triangular and rectangular splitter plates, for different Reynolds numbers. For the case of a single cylinder, convergence analysis demonstrated that accurate results can be achieved with a moderate number of basis functions. The observed relative errors fell below 1%, while the computational cost remained practical as each simulation requiring approximately 11 minutes on a standard workstation. Drag and lift coefficients were computed for the single-cylinder configuration and found to be in good agreement with established empirical data. This serves as quantitative validation of the method's accuracy and robustness in the low Reynolds number regime. For configurations with splitter plates, qualitative analysis revealed that the addition of the plate results in an effect similar to elongating the body in the direction of the flow. Elongated bodies, with their largest dimension oriented parallel to the main flow, tend to cause relatively narrow separated wakes, without generating a significant vortex wake. By installing splitter plates of various shapes and lengths in the near wake created by the body, it becomes possible to control the flow, for instance, to prevent the formation of a vortex street. Future studies could be

extended to cases with higher Reynolds numbers, more complex geometries, and unsteady flow regimes. Such extensions will help evaluate the generality and stability of the proposed approach across a broader class of fluid dynamics problems.

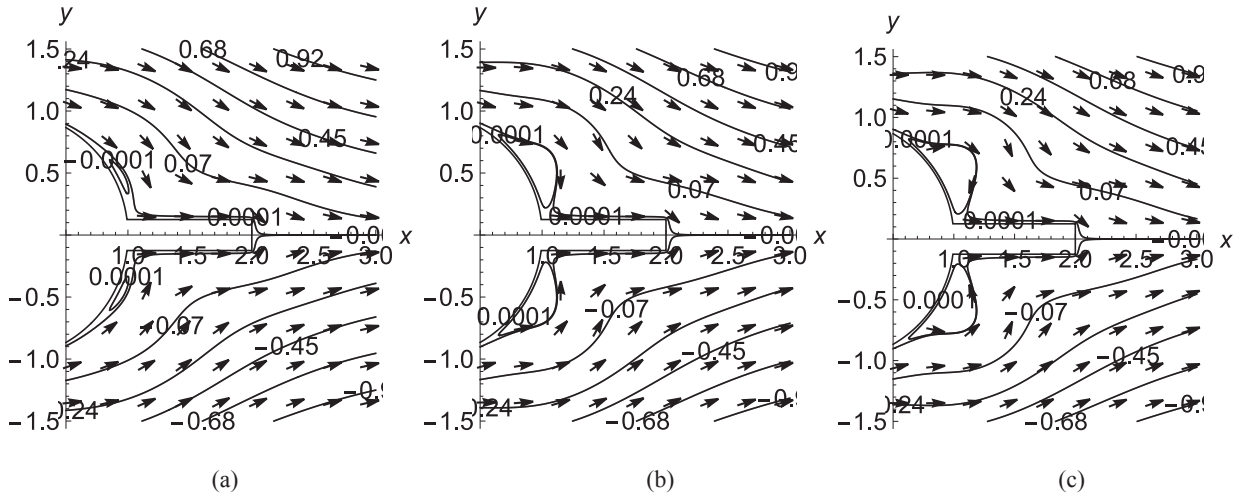

Figure 8 – Detailed visualizations of the streamline contours and velocity vector fields behind the circular cylinder with a rectangular splitter plate at (a) $\mathrm{Re} = 5$, (b) $\mathrm{Re} = 10$, (c) $\mathrm{Re} = 15$

References

1. Strelnikova, E., Choudhary, N., Degtyariov, K., Kriutchenko, D., and I. Vierushkin. "Boundary element method for hypersingular integral equations: Implementation and applications in potential theory." *Engineering Analysis with Boundary Elements* 169, Part B. 2024: 105999. https://doi.org/10.1016/j.enganabound.2024.105999.

2. Choudhary, N., Rana, S., Degtyarev, K., Kriutchenko D., and E. Strelnikova. "Numerical study on sloshing in coaxial shells." *Vibroengineering Procedia* 55. 2024: 86–90. https://doi.org/10.21595/vp.2024.24091.

3. Khoroshun, E., Makarov, V., Nehoduiko, V., Nechuiviter, O., Pershina, Y., and I. Veryovkin. "Mathematical modeling to predict the migration of foreign bodies of gunshot origin." *Emergency medicine* 20(5). 2024: 363–375. https://doi.org/10.22141/2224-0586.20.5.2024.1736.

4. Lytvyn, O., Zaluzhna, G., Nefodova, I., Pershyna, I., and O. Nechuiviter. "General Method for Constructing of the Exact Solution of the Problem for Non-Stationary Heat Conductivity Equation in the Complex Field." *Proceedings – International Conference on Advanced Computer Information Technologies, ACIT*. 2020: 144–147. https://doi.org/10.1109/ACIT49673.2020.9209005.

5. Happel, J., and H. Brenner. *Low Reynolds number hydrodynamics*. The Hague: Martinus Nijhoff Publishers, 1983. https://doi.org/10.1007/978-94-009-8352-6.

6. Loitsyansky, L.G. *Mechanics of liquids and gases*. New York: Begell House, 1995. https://doi.org/10.1615/978-1-56700-042-9.0.

7. Milne-Thomson, L.M. *Theoretical Hydrodynamics*. 5th edition. Dover Publications, 2011.

8. Polyanin, A.D., Kutepov, A.M., Kazenin, D.A., and A.V. Vyazmin. *Hydrodynamics, mass and heat transfer in chemical engineering*. London: CRC Press, 2001. https://doi.org/10.1201/9781420024517.

9. Shrivastava, V., Badami, P., Hiremath, N., Saravanan, V., and K.N. Seetharamu. "Numerical analysis of flow past circular cylinder with triangular and rectangular wake splitter." *International Journal of Mechanical, Industrial and Aerospace Sciences* 6(9). 2012: 1854–1861. https://doi.org/10.5281/zenodo.1327829.

10. Rvachov, V.L. *Theory of R-functions and their applications*. Kyiv: Nauk. Dumka, 1982.

11. Shapiro, V. "Semi-analytic geometry with *R*-functions." *Acta Numer*. 16. 2007: 239–303. https://doi.org/10.1017/S096249290631001X.

12. Maksimenko-Sheyko, K.V., Uvarov, R.A., and T.I. Sheyko. "The *R*-functions method in mathematical modeling of convective heat transfer in fuel cartridge with fuel rods." *Problems of Atomic Science and Technology* N3(85). Series: Nuclear Physics Investigations (60). 2013: 205–209.

13. Kolyada, R.A., Maksimenko-Sheiko, K.V., and T.I. Sheiko. "*R*-Functions Method in the Mathematical Modeling of Convective Heat Exchange in an Octahedral Fuel Assembly with 37 Fuel Elements." *J Math Sci* 238. 2019: 154–164. https://doi.org/10.1007/s10958-019-04225-w.

14. Sheyko T.I., Maksimenko-Sheyko K.V., Uvarov R.A., and M.A. Khazhmuradov. “The thermal-hydraulic calculation in a fuel cartridge when the symmetry of fuel rods packing is broken.” *Problems of Atomic Science and Technology* N3(121). Series: Nuclear Physics Investigations (71). 2019: 74–79.

15. Maksymenko-Sheiko, K.V., Sheiko, T.I., Lisin, D.O., and T.B. Dudinov. “Mathematical and Computer Modeling of Convective Heat Transfer in Fuel Cartridges of Fuel Elements with Different Shapes and Packing of Rods.” *J. of Mech. Eng.* 25(1). 2022: 40–54. https://doi.org/10.15407/pmach2022.01.040.

16. Podhornyj O.R., and M.V. Sidorov. “Mathematical modeling of fluid flows through the piecewise homogeneous porous medium by *R*-function method.” *Mathematical Modeling and Computing* 8(3). 2021: 499–508. https://doi.org/10.23939/mmc2021.03.499.

17. Gybkina, N.V., Sidorov, M.V., and H.V. Stadnikova. “Mathematical modeling of the quasi-stationary processes of viscous mixture mixing in a rectangular area by the *R*-functions method.” *Bulletin of the National Technical University "KhPI". Ser. : System analysis, control and information technology* 2(8). 2022: 87–93. https://doi.org/10.20998/2079-0023.2022.02.14.

18. Lamtyugova, S.N., and M.V. Sidorov. “Numerical analysis of the external slow flows of a viscous fluid using the *R*-function method.” *Journal of Engineering Mathematics* 91(1). 2015: 59–79. https://doi.org/10.1007/s10665-014-9746-x.

19. Lamtyugova, S.N. “Mathematical modelling of flow linearized problems in the spherical and cylindrical coordinate systems.” *Visn ZNU. Ser. Fiz. Math. Nauky* 1. 2012: 112–122.

20. Lamtyugova, S.N., and M.V. Sidorov. “The *R*-functions method application to numerical analysis of flow problem in a cylindrical coordinate system.” *Bulletin of V. Karazin Kharkiv National University. Series “Mathematical Modelling. Information Technology. Automated Control Systems”* 1105(24). 2014: 111-121.

21. Lamtyugova, S.N., Sidorov, M.V., and I.V. Sytnykova. “Method of numerical analysis of the problem of mass transfer of a cylindrical body with the uniform translational flow.” *Radio Electronics, Computer Science, Control* 2. 2018: 22–29. https://doi.org/10.15588/1607-3274-2018-2-3.

22. Polyanin, A.D., and V.F. Zaitsev. *Handbook of Nonlinear Partial Differential Equations*. 2nd edition. New York: Chapman and Hall/CRC, 2012. https://doi.org/10.1201/b11412.

23. Perumal, D.A., Kumar, G.V.S., and A.K. Dass. “Lattice Boltzmann simulation of flow over a circular cylinder at moderate Reynolds numbers.” *Thermal Science* 18(4). 2014: 1235–1246. https://doi.org/10.2298/TSCI110908093A.

24. Dennis, S.C.R., and G.-Z. Chang. “Numerical solutions for steady flow past a circular cylinder at Reynolds numbers up to 100.” *J. Fluid Mech.* 42(3). 1970: 471–489. https://doi.org/10.1017/S0022112070001428.

25. Chhabra, R. P. and S. A. Patel. *Bubbles, Drops, and Particles in Non-Newtonian Fluids*. 3 ed. Taylor & Francis, 2023.

26. Baracu, T. and R. Boşneagu. “Numerical analysis of the flow around a cylinder for the perspective of correlations of the drag coefficient of the ship’s hulls.” *Scientific Bulletin of Naval Academy*. Vol. XXII. 2019: 256–267.

27. Silva, A., Silveira-Neto, A. and J. J. Damasceno. “Numerical simulation of two-dimensional flows over a circular cylinder using immersed boundary method.” *Journal of Computational Physics*. 189. 2003: 351–370. https://doi.org/10.1016/S0021-9991(03)00214-6.

28. Yuce, M. and D. Kareem. “A Numerical Analysis of Fluid Flow Around Circular and Square Cylinders.” *American Water Works Association*. 108. 2016: 546 – 554. https://doi.org/10.5942/jawwa.2016.108.0141.

Author Biography:

Svitlana Mykolayivna Lamtiuhova – PhD in Physics and Mathematics, Associate Professor of Applied Mathematics Department, Kharkiv National University of Radio Electronics, Nauky Ave. 14, Kharkiv, Ukraine, svitlana.lamtiuhova@nure.ua